Journal of Macromolecular Science, Part A
Publication details, including instructions for authors and subscription information:
http://www.informaworld.com/smpp/title~content=t713597274

Novel Preparation of Polyethylene from Nano-extrusion Polymerization Inside the Nanochannels of MCM-41/$MgCl_2$/$TiCl_4$ Catalysts

Mohammad Ali Semsarzadeh[a]; Alireza Aghili[a]
[a] Polymer Engineering Group, Tarbiat Modares University, Tehran, Iran

To cite this Article Semsarzadeh, Mohammad Ali and Aghili, Alireza(2008) 'Novel Preparation of Polyethylene from Nano-extrusion Polymerization Inside the Nanochannels of MCM-41/$MgCl_2$/$TiCl_4$ Catalysts', Journal of Macromolecular Science, Part A, 45: 8, 680 — 686

To link to this Article: DOI: 10.1080/10601320802170450

URL: http://dx.doi.org/10.1080/10601320802170450

Journal of Macromolecular Science®, Part A: Pure and Applied Chemistry (2008) **45**, 680–686

ISSN: 1060-1325 print/1520-5738 online
DOI: 10.1080/10601320802170450

Novel Preparation of Polyethylene from Nano-extrusion Polymerization Inside the Nanochannels of MCM-41/$MgCl_2$/$TiCl_4$ Catalysts

MOHAMMAD ALI SEMSARZADEH and ALIREZA AGHILI
Polymer Engineering Group, Tarbiat Modares University, Tehran, Iran

Received October, 2007, Accepted January, 2008

The MCM-41 and SiO_2 supported $TiCl_4$ and $TiCl_4$/$MgCl_2$ catalysts with different molar ratios of Mg/Ti were synthesized and used for ethylene polymerization under atmospheric pressure. The nanochannels of MCM-41 serve as nanoscale polymerization reactor and the polyethylene nanofibers were extruded during the reaction. The nanofibers were observed in SEM micrographs of resulting polyethylene. The effect of $MgCl_2$ on catalytic activity and thermal properties of resulting polyethylene is investigated too. In the presence of $MgCl_2$, the catalytic activity increased and more crystalline polyethylene with higher melting points were formed. However, no fibers could be observed in the polyethylene prepared by SiO_2 supported catalysts.

Keywords: polyethylene nanofiber; nano-extrusion polymerization; Ziegler-Natta catalyst; atmospheric pressure

1 Introduction

The production of polyolefins in recent years is continuously growing and predicted to rise at a high rate. Intense research has been carried out on olefin polymerization catalysis, in order to develop new catalytic systems capable of producing new materials, as well as developing more economic and versatile processes. Different kinds of metal halides or oxides have been used as support of catalyst for olefin polymerization. $MgCl_2$ has been reported as a good support for preparation of highly active Ziegler–Natta catalysts. Inorganic compounds such as silica and alumina, when used as support of polymerization catalysis, have an important role in controlling the morphology of growing polymer particles, due to a large surface area and wide range of pores size distribution. It is possible to control the catalytic activity, as well as morphology of growing particles by using bi-supported Ziegler–Natta catalysts. Three different ways have been reported for preparation of SiO_2/$MgCl_2$ bisupported $TiCl_4$ catalysts. The first method is to mix an alcoholate solution of $MgCl_2$ with pretreated SiO_2 in a non-polar solvent, and further treating with $TiCl_4$ solution (1). The second method is to prepare the catalyst by mixing $TiCl_4$ solution with pretreated SiO_2, then treating with THF solution of $MgCl_2$ (2). In the third method, the catalyst is prepared by anchoring Ti/Mg bimetallic complex to the surface of silica, through treating THF solution of $MgCl_2$/$TiCl_4$ with pretreated SiO_2 (3). The mode of reaction between the hydroxyl groups of silica and bimetallic halides will affect the catalytic activity of the catalyst (3). To control the morphology of the resulting polymer, mesoporous materials with constrained geometries can be expected to be suitable supports for catalyst preparation. To this end, many attempts have been made to prepare the Si and/or Al based mesoporous structures with a larger surface area and more uniform pore size distribution than conventional silica and/or alumina. Mesoporous Silica Fiber (MSF), Mobil Composition of Matter (MCM-41), Santa Barbara Amorphous (SBA-15), Anodized Aluminum Oxide (AAO) and alumino-silicate (Al-MCM-41, Al-SBA-15) structures, with regular, ordered hexagonal pores and narrow pore size distribution, are some examples which have been used as support for preparing heterogeneous catalysts. The geometrical shape of the nanochannels can serve as nanoscale polymerization reactors (4, 5) to affect the pattern of monomer insertion and to control polymer chain structure and morphology. Polyethylene nanofibers, a new morphology of synthesized polymers, were prepared for the first time by Aida et al. (6) with MSF supported titanocene catalyst via a polymerization process termed as extrusion polymerization. Ye et al. (7) showed that the nanofibers prepared by MCM-41 supported Cp_2TiCl_2 have special mechanical properties.

Address correspondence to: M. A. Semsarzadeh, Polymer Engineering Group, Tarbiat Modares University, Jalal Al-e-Ahmad highway, Tehran, P.O. Box: 14115-111, Iran. Tel.: +98 21 82 88 33 39; E-mail: semsarzadeh@modares.ac.ir

MCM-41, SBA-15, AAO and alumino-silicate structures have been used as a support of metallocene and Ziegler–Natta catalysts for polymerization of ethylene or propylene (5, 7, 8–22). The major morphology of polymers prepared by these catalytic systems is polyethylene nanofibers or confined PE and PP.

In this work, MCM-41 supported $TiCl_4$ and $TiCl_4/MgCl_2$ catalysts were synthesized by anchoring Ti/Mg bimetallic complex into the nanochannels of MCM-41. These catalysts were used for preparation of polyethylene nanofibers via ethylene extrusion polymerization under atmospheric pressure. These catalytic systems were compared to $SiO_2/TiCl_4$ and $SiO_2/MgCl_2/TiCl_4$ under the same conditions of catalyst preparation and ethylene polymerization. The effect of supports and $MgCl_2$ on catalytic activities and melting points and crystallinity and morphology of the resultant polyethylene were investigated.

2 Experimental

2.1 Materials

All manipulations involving air and/or water sensitive compounds were performed under nitrogen atmosphere. *n*-hexadecyltrimethylammonium bromide, aqueous ammonia (reagent grade 25 wt%), Titanium tetrachloride, anhydrous magnesium chloride and tetrahydrofuran were purchased from Merck. Tetraethoxysilane (TEOS) was purchased from Acros. Triethylaluminium ($AlEt_3$) and SiO_2 were purchased from Aldrich. Polymerization-grade ethylene and nitrogen, both with purity of 99.999% were passed through columns of silica gel, 3 and 4 Å molecular sieves. After distillation, hexane was refluxed over sodium wire with benzophenone as an indicator and distilled again before use.

2.2 Preparation of MCM-41

2.4 g of *n*-hexadecyltrimethylammonium bromide (0.0066 mol) as a template was dissolved in 120 g deionized water, and 9.5 g of aqueous ammonia (25 wt%, 0.14 mol) was added to the solution. While stirring, 10 g of tetraethoxysilane (0.05 mol) was added slowly to the surfactant solution over a period of 15 min resulting in a gel. The mixture was stirred for 1 h, and then the white precipitate was filtered and washed with deionized water. After drying at 90°C for 12 h, the sample was heated to 550°C (rate:1°C/min) in air and kept at this temperature for 5 h to remove the template (23).

2.3 Preparation of Catalyst Systems

The support (MCM-41 or SiO_2) powders were treated in flowing ultra high-purity nitrogen at 400°C for 9 h before use in catalyst preparation. To a 250-ml double-walled glass reactor equipped with a glass stirring bar and connected to a constant temperature circulator, were added 2.0 g of support and 0.2 g $TiCl_4$ solution in hexane at room temperature. After raising the temperature to 55°C, the mixture was stirred for 3 h, filtered and washed with plenty of hexane under nitrogen atmosphere. Alternatively, to a 250 ml round bottom flask containing 50 ml of electron donor (THF) was added an appropriate amount of anhydrous $MgCl_2$. The mixture was kept standing with vigorous stirring until $MgCl_2$ was completely dissolved at 60°C. This mixture was transferred to the glass reactor and a 2.0 g $TiCl_4$ solution in hexane was added dropwise at 55°C over 15 min to this mixture. This yellow precursor was impregnated to 2.0 g support and was kept under stirring for 3 h, filtered and washed with hexane under nitrogen atmosphere.

2.4 Ethylene Polymerization

The ethylene polymerization was carried out in a 250 ml round bottom flask with a Teflon stirrer under atmospheric pressure. Hexane and catalyst were added into the flask. The mixture was saturated with ethylene and stirred for a few minutes. At the temperature of 50°C, polymerization was initiated by adding an appropriate amount of $AlEt_3$ to the reactor. The reaction was terminated at a fixed time by adding a dilute hydrochloric acid solution in methanol. The polymer was filtered and then dried at 60°C overnight.

2.5 Characterization of Support

The thermogravimetric analyses (Perkin-Elmer Pyris1) of the dried sample was carried out in air to simulate the calcination process in the oven during the preparation of MCM-41. The X-ray powder diffraction spectra were recorded on a Philips X'pert diffractometer. The nitrogen adsorption–desorption isotherms were measured at BELSORP-mini adsorption apparatus. The specific surface area of support was obtained based on the BET (Brunauer, Emmett, and Teller) method. The pore size distribution was calculated using a BJH (Barrett–Joyner–Halenda) method. A scanning electron microscopy (Philips XL30) was used for investigating the morphology of support.

2.6 Characterization of Polymer

A differential scanning calorimetry analysis (DSC) was carried out on a NETZSCH DSC 200 F3 instrument with a heating rate of 10°C/min from 25 to 180°C under a nitrogen atmosphere. The results of the first scan are reported here. The XRD spectra of the polymers were recorded on a Philips X'pert diffractometer. The morphology of the polymers was observed on a scanning electron microscopy (Philips XL30). The polymers were deposited on a sample holder and sputtered with gold. Molecular weights of the polymers were measured with a capillary viscometer. The measurements were carried out at 180.1°C, using 1-octanol as θ-solvent in this temperature. The viscosity-average molecular weight can be calculated according to

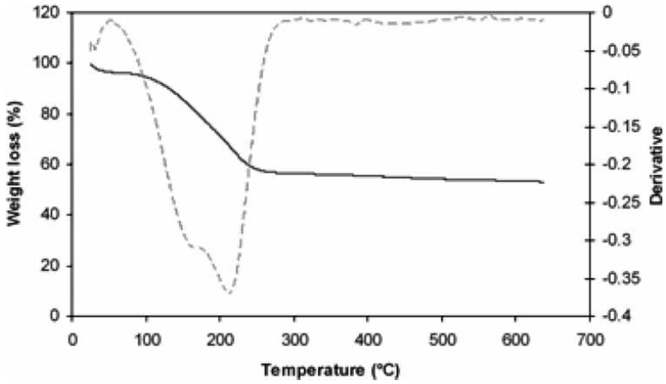

Fig. 1. The TG and DTG curves for MCM-41 support.

the Mark-Houwink-Sakurada equation:

$$[\eta] = KM_v^a$$

where $[\eta]$ is intrinsic viscosity, $K = 28.6 \times 10^{-4}$ dL g^{-1} and $a = 0.5$ are the constants for polyethylene and 1-octanol at θ temperature (24).

3 Results and Discussion

3.1 Characterization of MCM-41

The thermogravimetric analysis of the dried sample at 90°C for 12 h, showed that after 90°C, water and organics are released or burned from the structure in two main steps (Fig. 1), at 90–180 and 180–300°C. The steps may relate to the removal of water inside the pores or crystal structure and the combustion of the template, respectively (25). The weight loss at higher temperatures (>300°C) is due to the burning of the rest of the organics and/or the loss of water released as a result of condensation of silanol groups to siloxane bonds (25).

X-ray diffraction (XRD) and nitrogen adsorption–desorption isotherm were used to characterize the internal structure of the MCM-41. Figure 2 shows the XRD spectra of the MCM-41. The characteristic Bragg peaks with *d*-spacings 30.8, 18.3, and 15.6 Å at 2.86, 4.83 and 5.66° 2θ correspond to reflections from the [100], [110] and [200] planes, respectively (23). No characteristic peak was observed in the XRD patterns of SiO_2 and so it has an amorphous structure.

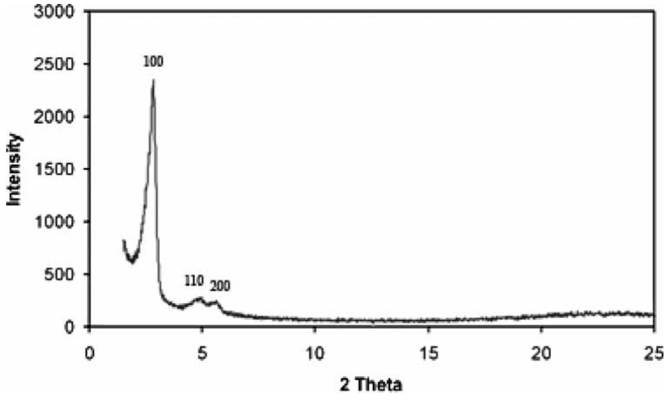

Fig. 2. X-ray diffraction patterns of MCM-41.

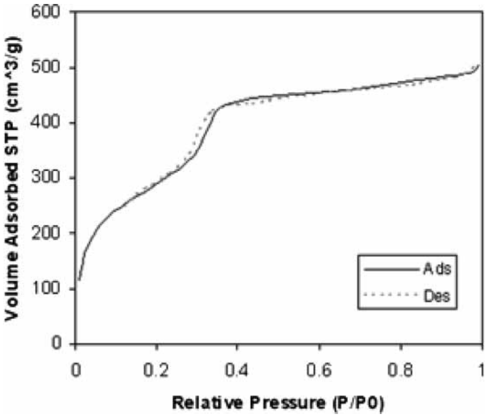

Fig. 3. Nitrogen adsorption–desorption isotherm of MCM-41.

Figure 3 shows the nitrogen adsorption–desorption isotherm of the MCM-41. The adsorption and desorption isotherms of nitrogen on the sample show the typical type IV isotherm according to the IUPAC nomenclature for MCM-41 (23). Table 1 summarizes the structure parameters of the MCM-41, including specific surface area, average pore diameter, pore volume and XRD interplanar spacing, from the nitrogen adsorption–desorption and XRD analyses. For comparison, the specific surface area, average pore diameter and pore volume of SiO_2 are shown in Table 1, which are taken from manufacturer's data.

Figure 4 (a) and (b) show the SEM micrograph of MCM-41 and SiO_2, respectively. The MCM-41 has rod-like structure of about 1–3 μm in length and about 0.5 μm in diameter. Each particle consisted of thousands to millions of hexagonal nanochannels (7). As reported by manufacturer, SiO_2 has particles with diameter of 5–25 μm.

3.2 Characterization of Catalysts

Titanium and magnesium loadings on the supports were determined by Inductively Coupled Plasma–Mass Spectroscopy (ICP-MS). The results are shown in the Table 2. MCM-41 has a larger surface area than SiO_2 and more –OH groups per mass unit of supports are present on the surface for reaction with $TiCl_4$ or $TiCl_4/MgCl_2$ bimetallic

Table 1. Structure parameters for the supports

Support[a]	S_{BET} (m^2/g)	V_p (ml/g)	d_p (Å)	d_{100} (Å)
MCM-41[b]	1070	0.78	29.2	30.8
SiO_2[c]	~500	0.75	60	—

[a] S_{BET}, BET specific surface area; V_p, specific pore volume; d_p, average pore diameter; d_{100}, XRD interplanar spacing.

[b] Data from nitrogen sorption.

[c] Data from manufacturer.

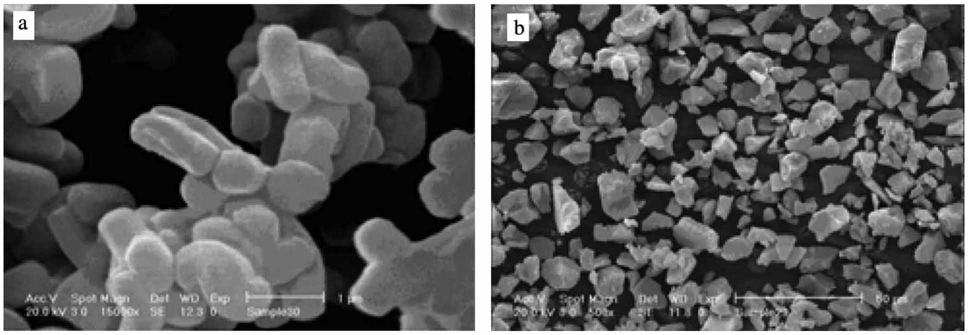

Fig. 4. SEM micrograph of the (a) MCM-41 and (b) SiO_2.

complexes. So it is evident that more Ti and Mg are chemisorbed on the surface of MCM-41.

3.3 Ethylene Polymerization

The MCM-41 and SiO_2 supported $TiCl_4$ and $TiCl_4/MgCl_2$ catalysts were used for ethylene polymerization. Table 3 shows the polymerization results and polymer properties. The MCM-41 supported catalysts showed higher activities than the SiO_2 supported catalysts. $MgCl_2$ has enhanced the activities of both supported catalysts. The rate enhancement effect of $MgCl_2$ in silica supported catalysts has been well discussed in the literature (1–3, 26, 27). $TiCl_4$, in the presence of $MgCl_2$, forms bimetallic complexes which are chemisorbed on the surface of support and have higher activities than the case that $TiCl_4$ is used alone. The results of DSC analysis show that the polyethylenes prepared by MCM-41 supported catalysts have higher melting points and ΔH in comparison to SiO_2 supported catalysts. This indicates that the nanochannels of MCM-41 can control the direction of the chain propagation to increase the crystallinity of the polyethylene (21). It was also found that $MgCl_2$ increased the melting point and crystallinity of polyethylene prepared by MCM-41 supported catalysts. Viscosity average molecular weights of polymers show that the polymers prepared by MCM-41 have higher molecular weight compared to that of SiO_2. These results

Table 2. Chemisorbed elements on the catalysts

Run	Catalyst	Mole ratio[a] Mg/Ti	Ti content (mmol/ g-cat)	Mg content (mmol/ g-cat)
1	$SiO_2/TiCl_4$	0	0.134	—
2	$SiO_2/MgCl_2/TiCl_4$	0.5	0.140	0.062
3	$SiO_2/MgCl_2/TiCl_4$	1	0.133	0.110
4	$SiO_2/MgCl_2/TiCl_4$	2	0.126	0.198
5	$MCM\text{-}41/TiCl_4$	0	0.151	—
6	$MCM\text{-}41/MgCl_2/TiCl_4$	0.5	0.160	0.064
7	$MCM\text{-}41/MgCl_2/TiCl_4$	1	0.154	0.123
8	$MCM\text{-}41/MgCl_2/TiCl_4$	2	0.163	0.232

[a] Used in catalysts preparation.

Table 3. Ethylene polymerization using supported catalysts[a]

Run	Catalyst	Mole Ratio Mg/Ti	Activity (10^4 g PE/mol-Ti h)	T_m[b] (°C)	$-\Delta H$[c] (J/g)	M_v (10^5 g/mol)
1	$SiO_2/TiCl_4$	0	0.37	134.5	104.2	1.32
2	$SiO_2/MgCl_2/TiCl_4$	0.5	1.01	135.4	110.1	1.22
3	$SiO_2/MgCl_2/TiCl_4$	1	1.78	134.3	107.1	1.17
4	$SiO_2/MgCl_2/TiCl_4$	2	2.91	135.2	108.4	1.28
5	$MCM\text{-}41/TiCl_4$	0	0.82	139.2	176.8	4.61
6	$MCM\text{-}41/MgCl_2/TiCl_4$	0.5	1.59	139.9	194.4	4.72
7	$MCM\text{-}41/MgCl_2/TiCl_4$	1	2.70	140.7	188.4	5.12
8	$MCM\text{-}41/MgCl_2/TiCl_4$	2	4.74	142.5	197.3	4.93

[a] Solvent = hexane (100 ml), Al/Ti molar ratio = 30, polymerization pressure = 1 atm, Temperature = 50°C, Time = 30 min.
[b] Data from first scan.
[c] Per gram of polymer.

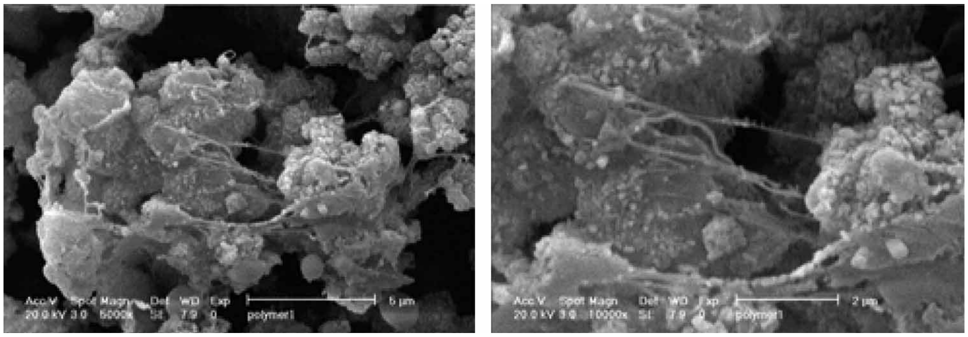

Fig. 5. SEM micrograph of the polyethylene prepared by MCM-41/$TiCl_4$ catalyst.

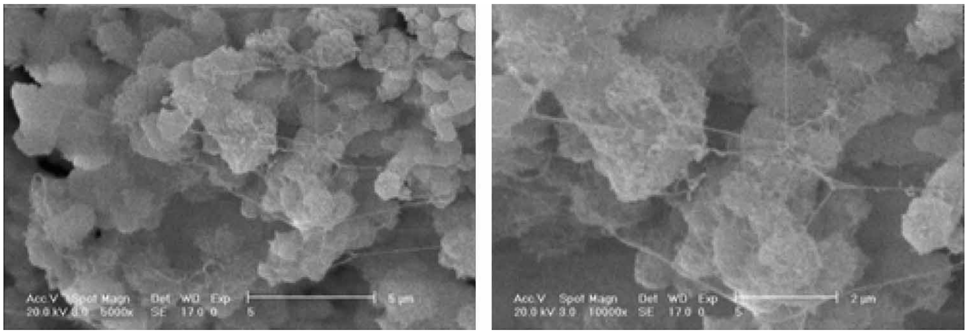

Fig. 6. SEM micrograph of the polyethylene prepared by MCM-41/$MgCl_2$/$TiCl_4$ catalyst (Mg/Ti = 0.5).

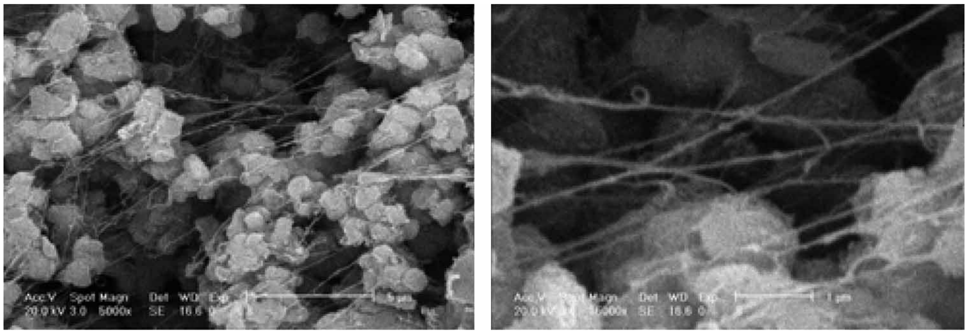

Fig. 7. SEM micrograph of the polyethylene prepared by MCM-41/$MgCl_2$/$TiCl_4$ catalyst (Mg/Ti = 1).

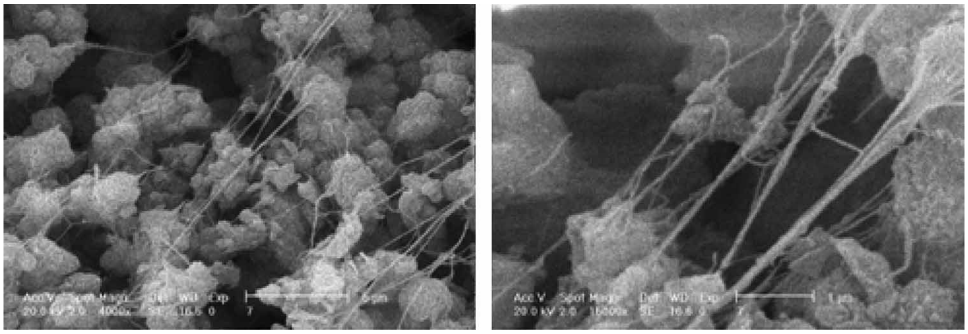

Fig. 8. SEM micrograph of the polyethylene prepared by MCM-41/$MgCl_2$/$TiCl_4$ catalyst (Mg/Ti = 2).

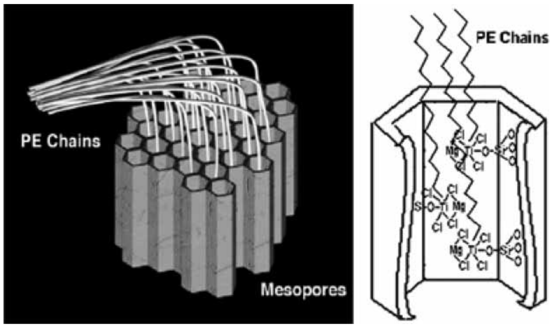

Fig. 9. Conceptual scheme for the growth of crystalline fibers of polyethylene.

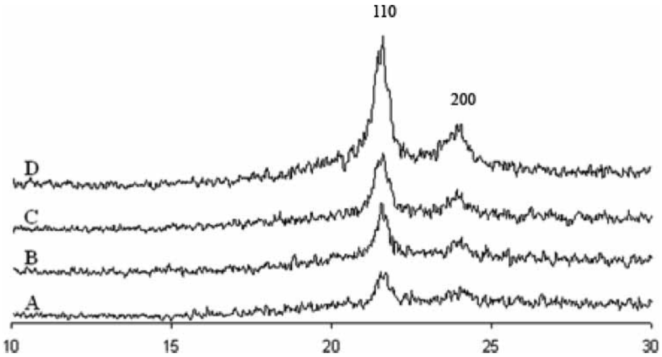

Fig. 10. XRD patterns of PE prepared by MCM-41/$MgCl_2$/$TiCl_4$ catalysts with molar ratios Mg/Ti of (A) 0, (B) 0.5, (C) 1 and (D) 2.

suggest a possible elongation of the propagating polymer chain within the mesoporous channels, as described by Kageyama et al. (12).

3.4 *The morphology of the Resulting PE*

Morphological investigation of the resulting PE was conducted with SEM. Figure 5 shows the SEM micrographs of the resulting PE prepared by the MCM-41/$TiCl_4$ catalyst. These figures show that the PE mainly has amorphous morphology and a few fibers appear on the surface of the amorphous PE. Figures 6, 7 and 8 show the SEM micrograph of PE prepared by MCM-41/$MgCl_2$/$TiCl_4$ catalysts with Mg/Ti molar ratios of 0.5, 1 and 2, respectively. When $MgCl_2$ was used in MCM-41 supported catalysts, the polymers have still fibrous morphology.

The PE nanofibers result from the control of MCM-41 nanochannels to the direction and dimension of PE chains propagation (20). MCM-41 consists of a honeycomb shaped array of unidimensional, hexagonal pores (20) and the pore diameter (29 Å) is much smaller than the lamellar thickness (270 Å) of the folded-chain crystals of ordinary polyethylene (28). Therefore, formation of PE nanofibers from the nanochannels may take laminar thickness of almost 1/10 of this ordinary structure. When the ethylene monomers pass into the channel, the wall of the channel can control the direction of ethylene propagation and the PE extended-chains are formed. Then, these extended-chains grow out of MCM-41 nanochannels and assemble to form nanofibers (Fig. 9) (6).

The crystalline structure of polyethylene nanofibers have been studied by XRD analysis in the literature (6, 7, 10, 16, 19, 29). The XRD spectra of the resultant polymer, including the polyethylene and the supports, in Fig. 10, show a typical orthorhombic crystal structure for the crystalline PE with [110] and [200] diffraction peaks at 21.2° and 24°, respectively. The amorphous halo around 19.6, for all the samples, is negligibly small, indicating the high crystallinity (7) of the polymer samples prepared by different molar ratios of Mg/Ti.

Figure 11 (a) and (b) show the micrographs of PE prepared by SiO_2/$MgCl_2$/$TiCl_4$ and SiO_2/$TiCl_4$ catalysts, respectively. It was found that the PE only has amorphous morphology and no fibers present.

As is known to us, MCM-41 was used as support for metallocene catalysts for the preparation of polyethylene nanofibers (7, 11, 19, 20). Wang and coworkers (21) used MCM-41 for $TiCl_4$ Ziegler–Natta catalyst. They have found that the resulting PE prepared by MCM-41 supported catalyst leads to an amorphous polyethylene with a few nanofibers on the surface of PE particles. They showed that the polyethylene nanofibers could be synthesized when the active sites on the exterior surface of MCM-41 were destroyed by hydroxyl groups in β-cyclodextrin, besides the

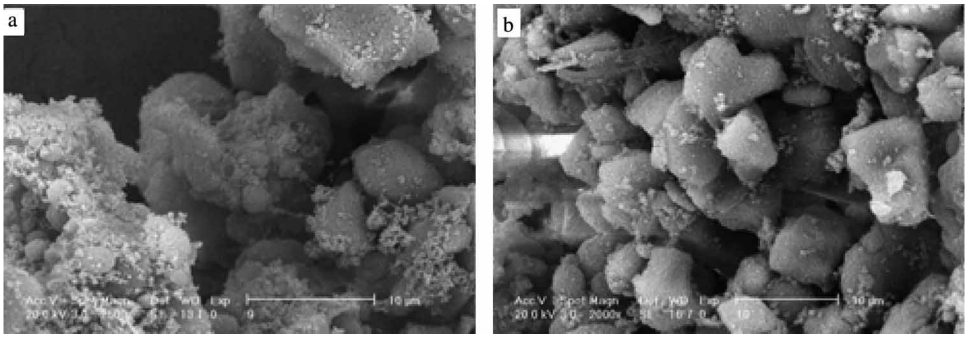

Fig. 11. SEM micrograph of the polyethylene prepared by (a) SiO_2/$MgCl_2$/$TiCl_4$ (Mg/Ti = 2) and (b) SiO_2/$TiCl_4$ catalyst.

fact that the activity of catalytic system decreased. Zhang and co-workers (22) synthesized MCM-41/$MgCl_2$/$TiCl_4$ catalyst by treating $MgCl_2$/n-butanol homogeneous solution to MCM-41 and further treating with $TiCl_4$ solution. They have also found that the existence of $MgCl_2$ could increase the polymerization rate and make the resultant polyethylene have fibrous morphology. We synthesized MCM-41/$MgCl_2$/$TiCl_4$ Ziegler-Natta catalysts with different Mg/Ti molar ratios, by anchoring Ti/Mg bimetallic complex into the nanochannels of MCM-41 and used these catalytic systems for preparation of polyethylene nanofibers under atmospheric pressure. We showed that $MgCl_2$ could increase the catalytic activity, as well as melting points of crystalline fibrous polyethylene.

4 Conclusions

MCM-41 and SiO_2 supported $TiCl_4$ and $TiCl_4$/$MgCl_2$ catalysts were synthesized for ethylene polymerization under atmospheric pressure. The active sites formed inside the nanochannels of MCM-41. Ethylene monomer diffused into the channels and growing polyethylene chains were extruded to form nanofibers. MCM-41 showed higher activity than SiO_2 supported catalysts. $MgCl_2$ has enhanced the catalytic activities of both supports. The resulting PE prepared by MCM-41 supported catalysts have larger melting points, crystallinity and molecular weights than that of SiO_2 supported catalysts.

5 Acknowledgment

We would like to thank the Center of Excellence for Chemical Engineering Processes at Tarbiat Modares University for the financial support of this project.

6 References

1. Lu, H. and Xiao, S. (1993) *Makromol. Chem.*, **194(2)**, 421–429.
2. de Santa Maria, L.C., Soga, K. and Shiono, T. (1994) *Macromol. Chem. Phys.*, **195(7)**, 2591–2598.
3. Kim, I., Kim, J.H. and Woo, S.I. (1990) *J. Appl. Polym. Sci.*, **39(4)**, 837–854.
4. Lehmus, P. and Rieger, B. (1999) *Science*, **285(5436)**, 2081–2082.
5. Sano, T. and Yasunori, O. (2004) *Catal. Surv. Asia.*, **8(4)**, 295–304.
6. Kageyama, K., Tamazawa, J. and Aida, T. (1999) *Science*, **285(5436)**, 2113–2115.
7. Ye, Z., Zhu, S., Wang, W.J., Alsyouri, H. and Lin, Y.S. (2003) *J. Polym. Sci., Part B. Polym. Phys.*, **41(20)**, 2433–2443.
8. Turunen, J.P.J. and Pakkanen, T.T. (2007) *J. Molecul. Catalys. A: Chem.*, **263(1–2)**, 1–8.
9. Dong, X., Wang, Li., Wang, J., Zhou, J. and Sun, T. (2006) *J. Phys. Chem. B*, **110(18)**, 9100–9104.
10. Nair, S., Naredi, P. and Kim, S.H. (2005) *J. Phys. Chem. B*, **109(25)**, 12491–12497.
11. Chen, S., Guo, C., Liuc, L., Xu, H., Dong, J. and Hu, Y. (2005) *Polym.*, **46(24)**, 11093–11098.
12. Kageyama, K., Ng, S.M., Ichikawa, H.I. and Aida, T. (2000) *Macromol. Symp.*, **157(1)**, 137–142.
13. Guo, C., Zhang, D., Wang, F. and Jin, G.X. (2005) *J. Catal.*, **234(2)**, 356–363.
14. Turunen, J.P.J., Venäläinen, T., Suvanto, S. and Pakkanen, T.T. (2007) *J. Polym. Sci., Part A. Polym. Chem.*, **45(17)**, 4002–4012.
15. Guo, C., Jin, G.X. and Wang, F. (2004) *J. Polym. Sci., Part A. Polym. Chem.*, **42(19)**, 4830–4837.
16. Dong, X., Wang, L., Wang, W., Jiang, G., Chen, Y., Zhao, Z. and Wang, J. (2005) *Macromol. Mater. Eng.*, **290(1)**, 31–37.
17. Nakajima, H., Yamada, K., Iseki, Y., Hosoda, S., Hanai, A., Oumi, Y., Teranishi, T. and Sano, T. (2003) *J. Polym. Sci. part B. Polym. Phys.*, **40(24)**, 3324–3332.
18. Silveira, F., Petry, C.F., Pozebon, D., Pergher, S.B., Detoni, C., Stedile, F.C. and Santos, J.H.Z.D. (2007) *Appl. Catal. A: Gener.*, **333(1)**, 96–106.
19. Dong, X., Wang, L., Jiang, G., Zhao, Z., Sun, T., Yu, H. and Wang, W. (2005) *J. Molecul. Catalys. A: Chem.*, **240(1–2)**, 239–244.
20. Dong, X., Wang, L., Wang, W., Yu, H., Wang, J., Chen, T. and Zhao, Z. (2005) *Eur. Polym. J.*, **41(4)**, 797–803.
21. Dong, X., Wang, L., Zhou, J., Yu, H. and Sun, T. (2006) *Catalys. Commun.* (**1**), 1–5.
22. Zhang, W., Zhou, S. and Zhang, R. (2007) *Des. Monom. Polym.*, **10(5)**, 469–475.
23. Grün, M., Unger, K.K., Matsumoto, A. and Tsutsumi, K. (1999) *Micropor. Mesopor. Mater.*, **27(2–3)**, 207–216.
24. Mark, J.E. *Physical Properties of Polymers Handbook*, 2nd edn.; Mark, J.E. (ed.); Springer Science & Business Media, LLC: New york, Chap.15, p. 261, 2007.
25. Zhao, X.S., Lu, G.Q. and Millar, G.J. (1996) *Ind. Eng. Chem. Res.*, **35(7)**, 2075–2090.
26. Soga, K., Ohnishi, R. and Doi, Y. (1983) *Polym. Bull.*, **9(6–7)**, 299–304.
27. Rong, J., Jing, Z., Li, H. and Sheng, M. (2001) *Macromol. Rapid Commun.*, **22(5)**, 329–334.
28. Tajima, K. and Aida, T. (2000) *Chem. Commun.*, **24**, 2399–2412.
29. Ye, Z., Zhu, S. and Britten, J.F. (2006) *Macromol. Rapid Commun.*, **27(15)**, 1217–1222.